

Comparison ASL and DCE-MRI Perfusion Map in Small Animal Model of Cancer

^{1,2}L. Grossová, ¹R. Jiřík, ^{3,4}K. Souček, ^{1,5}E. Dražanová, ¹Z. Starčuk jr.

¹Institute of Scientific Instruments, AS CR, Brno, Czech Republic,

²Dept. of Biomedical Engineering, Brno Univ. of Technology, Brno, Czech Republic

³Dept. of Cytokinetics, Institute of Biophysics, AS CR, Brno, Czech Republic

⁴Center of Biomolecular and Cellular Engineering, International Clinical Research Center, St. Anne's Univ. Hospital Brno, Brno, Czech Republic

⁵Dept. of Medical Pharmacology, Faculty of Medicine MU, Brno, Czech Republic

Email: grossoval@isibrno.cz

Abstract. *This paper is focused on quantitative perfusion analysis using pulsed ASL (FAIR-RARE) and DCE-MRI (using high- and low-molecular-weight contrast agents) in a mouse tumour model. Tumour blood-flow maps of both methods were compared using visual assessment, region analysis (median, percentiles), scatter plots and correlation coefficients. ASL blood-flow estimates matched the DCE-MRI blood-flow estimations in some cases. Possible reasons for poor match in the other cases were investigated. This study indicates that in tumour perfusion analysis, we might profit from the combination of ASL and DCE-MRI instead of using just one of them.*

Keywords: Blood Flow Quantification, ASL, DCE-MRI, Perfusion, Tumour

1. Introduction

Blood flow imaging is an important tool, especially in oncology, neurology and cardiology. Magnetic resonance imaging (MRI) provides three quantitative methods of blood flow imaging: Dynamic Susceptibility Contrast MRI (DSC-MRI, contrast-agent based, mostly for brain applications), Dynamic Contrast-enhanced MRI (DCE-MRI, contrast-agent based, mostly for tumour applications) and Arterial Spin Labeling (ASL, no contrast agent, mostly for brain applications). In studies focused on brain imaging, ASL was compared to DSC-MRI. In recent years, several studies comparing ASL vs. DCE-MRI appeared due to an expansion of ASL from brain applications also to other organs (kidneys [1], pulmonary parenchyma [2], tumour-treatment response [3]). These studies indirectly compared blood flow estimated with ASL to the perfusion parameters estimated by DCE-MRI (k_{ep} , K^{trans} , v_e) which are only related to blood flow but not equivalent. Our DCE-MRI method is based on advanced pharmacokinetic models providing estimates of blood flow. This provides a direct comparison of the same quantity, one estimated using ASL and one using DCE-MRI. Also, compared to the previous approaches, here we do not intend to replace one method by another but aim at their combination to provide more reliable estimation of perfusion parameters.

2. Subject and Methods

Subjects

This study was evaluated on preclinical data from five BALB/c mice (approved by the animal care committees required by law). Murine colon tumour cells CT26.WT (ATCC, CTL-2638) were subcutaneously implanted into the left flank (1×10^6 cells in HC Matrigel). Each mouse underwent one ASL examination, and two DCE-MRI examinations, one with a high-molecular-weight contrast agent (Gadospin P, MiltenyiBiotec, BergischGladbach, Germany)

and one with a standard low-molecular-weight contrast agent (Magnevist, Bayer HealthCare Pharmaceuticals, Berlin, Germany).

MRI Acquisition

MR imaging was performed on mice using an experimental 9.4T Biospin (Bruker Biospin MRI, Ettlingen, Germany) scanner. A surface receiver coil and a volume transmitter coil were used. The mice were anesthetized with Isoflurane and O₂ mixture (2% of Isoflurane, 800ml/min of O₂). Their respiratory rate was monitored continuously during the whole measurement. The ASL sequence FAIR-RARE was used with the following acquisition parameters: 2D sequence with TR/TE 10 000/37.78 ms, image matrix 128×96 pixels, slice thickness 1 mm, FOV 23.2×35 mm, one axial slice through the tumour middle was imaged with 15 TI values (30, 50, 100, 200, 300, 500, 700, 900, 1000, 1100, 1500, 1800, 2200, 2800, 3200ms).

The acquisition parameters of DCE-MRI sequence were as follows: 2D FLASH sequence with TR/TE 14/2.5 ms, flip angle 25°, image matrix 128×96 pixels, slice thickness 1 mm, one axial slice (same as in ASL), sampling interval 1.05 s, acquisition time 13 min. Before the bolus administration, 15 pre-contrast images were recorded with 6 TRs (14, 30, 50, 100, 250, 500 ms) to convert the dynamic image sequence to the contrast-agent concentration. In addition, anatomical images were recorded using the RARE sequence (T₂-weighted and T₁-weighted pre- and post-contrast).

Data Analysis

All ASL data were analysed using the ParaVision software, version 5.1 (BrukerBrukerBiospin MRI, Ettlingen, Germany). ASL blood flow maps in manually drawn tumor ROIs were calculated with the following formula

$$F = \lambda \cdot \frac{T_{1nonsel}}{T_{1blood}} \left(\frac{1}{T_{1sel}} - \frac{1}{T_{1nonsel}} \right) \quad (1)$$

Where F is tissue blood flow [ml/min/g tissue], λ is the tissue-blood partition coefficient for water and T_{1sel} and T_{1nonsel} are longitudinal relaxation times of blood estimated using the selective or nonselective images, respectively.

All DCE-MRI data were analysed in MatlabTM (MathWorks, Nattick, USA). Adiabatic-approximation of the tissue homogeneity (ATH) pharmacokinetic model was used to model the tissue contrast-agent concentration time curves. Blind deconvolution was used for estimation of the arterial input function (part of the pharmacokinetic model) [4].

3. Results

Blood-flow maps from ASL and DCE-MRI data were first compared visually (Figs. 1, 2). For two mice (M1, M2), the maps were in a good agreement while for three mice (M3-M5) the maps did not match. Region analysis was done for manually drawn tumour ROIs for pixels where $v_e < 1$ (v_e – fractional interstitial volume estimated from DCE-MRI) to exclude necrotic regions where the pharmacokinetic model of DCE-MRI is not valid. The median and the 25th and 75th percentiles were calculated (Table 1). Scatter plots (Figs. 3) and the corresponding Pearson correlation coefficients were calculated to compare quantitatively the ASL and DCE-MRI results. To assess the validity of the DCE-MRI blood-flow estimates, an additional perfusion parameter estimated by DCE-MRI, *PS* (vessel permeability surface area product), was also reported (Table 1).

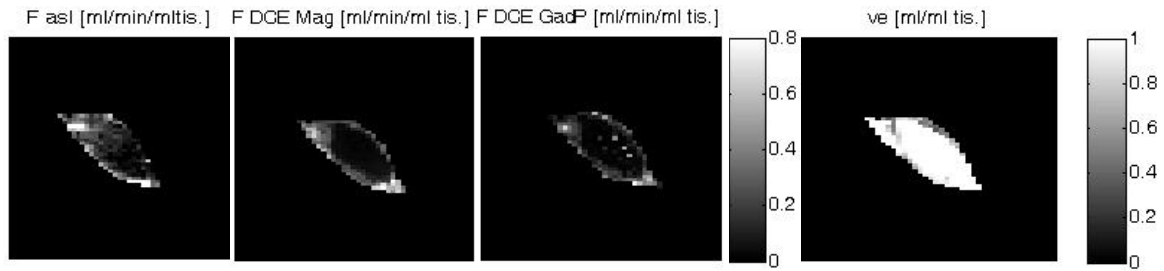


Fig. 1. Mouse M1 blood-flow maps, from the left ASL, DCE Magnevist, DCE GadospinP and ve.

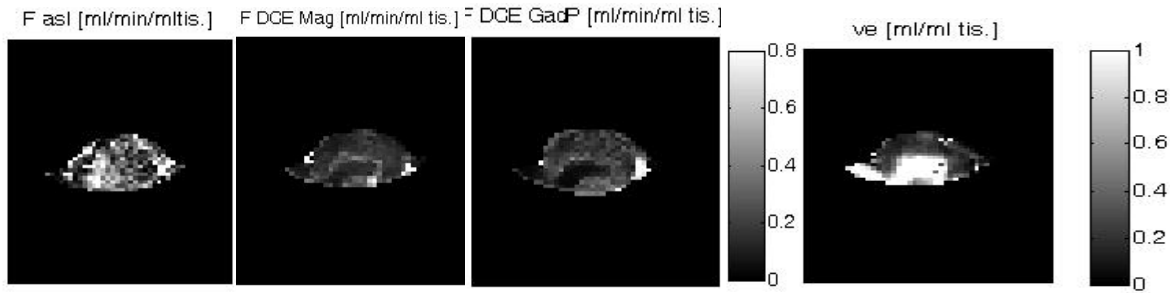


Fig. 2. Mouse M4 blood-flow maps, from the left ASL, DCE Magnevist, DCE GadospinP and ve.

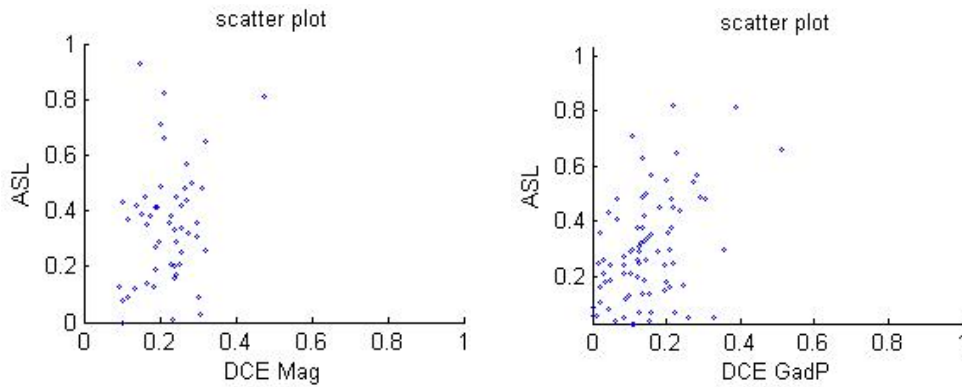


Fig. 3. Mouse M1 blood-flow scatter plots, left ASL vs. DCE (Magnevist), right ASL vs. DCE (GadospinP).

Table 1. Tables of blood-flow and PS median[25th; 75th percentiles], C - Pearson correlation coefficients, Mag - Magnevist, GadP - GadospinP, M - mouse.

M	F _{asl} [ml/min/g tis.]	F _{Mag} [ml/min/g tis.]	F _{GadP} [ml/min/g tis.]	PS _{Mag} [ml/min/g tis.]	PS _{GadP} [ml/min/g tis.]	C _{asl-Mag}	C _{asl-GadP}
1	0.25[0.1;0.6]	0.24[0.1;0.4]	0.13[0.1;0.2]	0.11[0.1;0.3]	0.03[0.01;0.07]	0.5	0.3
2	0.33[0.1;0.7]	0.31[0.1;0.5]	0.23[0.1;0.3]	0.15[0.1;0.2]	0.08[0.03;0.14]	0.4	0.3
3	0.34[0.1;1.0]	0.27[0.2;0.4]	0.21[0.1;0.3]	0.16[0.1;0.2]	0.10[0.07;0.15]	-0.02	0.1
4	0.36[0.1;0.7]	0.15[0.1;0.3]	0.16[0.1;0.2]	0.10[0.1;0.2]	0.06[0.04;0.09]	0.1	0.1
5	0.34[0.2;0.8]	0.26[0.2;0.4]	0.29[0.2;0.3]	0.11[0.1;0.2]	0.05[0.04;0.07]	-0.2	0.01

4. Discussion

The ASL and DCE blood-flow maps were consistent for mice M1 and M2, especially when comparing ASL to Magnevist DCE-MRI where the best match of blood flow medians and

Pearson correlation coefficients were obtained. This is in line with theoretical assumptions because GadoSpinP DCE-MRI data were noisier than Magnevist DCE-MRI data due to the limited extravasation of the high-molecular-weight contrast-agent. This was also shown by the approximately twofold decrease in the PS parameter. Furthermore, the low-flow areas corresponded well with the necrotic area indicated by high values in the v_e maps and bright areas in the post-contrast T_1 -weighted images. For mice M3 – M5, the agreement of ASL and DCE-MRI was poor because of several factors. First, the tumours were necrotic to a large extent, so the agreement could be evaluated only in few pixels. Another source of error might be seen in movement artefacts due to breathing, which were not so pronounced for M1 and M2. For mouse M4, ASL clearly failed (the T_1 quantification algorithm in the ParaVision software got trapped in a wrong estimate, checked by using own implementation). The reason for poor match in M3 and M5 is not completely clear. The above mentioned indirect measures of the DCE-MRI accuracy (consistency of PS and consistency of the flow maps with the v_e maps and post-contrast T_1 -weighted images) were similar as for mice M1, M2, suggesting that ASL failed also for these recordings.

5. Conclusions

The ASL perfusion analysis (using the ParaVision software, version 5.1) gave blood-flow values consistent with DCE-MRI (analysed using ATH pharmacokinetic model and blind deconvolution according to [4]) for two mice, while poor match was obtained for three other mouse experiments. The reasons for this mismatch will be analysed on a larger set of recordings with possibly larger highly perfused regions and less necrotic tissue. Our results also indicate a suboptimal reliability of the ASL-analysis part of the ParaVision software. This will be studied thoroughly as a follow-up work. The results indicate that it makes sense to combine ASL and DCE-MRI methods instead of using just one of them.

Acknowledgements

The study was supported by Ministry of Education, Youth, and Sports of the Czech Republic (project No. LO1212) and by the project FNUSA-ICRC (CZ.1.05/1.1.00/02.0123).

References

- [1] Cutajar M, Thomas D L, Hales P W, Banks T, Clarc Ch A, Gordon I. Comparison of ASL and DCE MRI for the non-invasive measurement of renal blood flow: quantification and reproducibility. *European Radiology*. 2014, vol. 24, issue 6, s. 1300-1308. DOI: 10.1007/s00330-014-3130-0.
- [2] Li F, Liu S, Sun F, Xiao X, Clarc CH A, Gordon I. Assessment of pulmonary parenchyma perfusion with FAIR in comparison with DCE-MRI—Initial results: quantification and reproducibility. *European Journal of Radiology*. 2009, vol. 70, issue 1, s. 41-48. DOI: 10.1016/j.ejrad.2007.12.013.
- [3] Wenchao C, Li F, Wang J, Huarui D, Wang X, Zhang J, Fang J, Jiang X. A comparison of arterial spin labeling perfusion MRI and DCE-MRI in human prostate cancer. *NMR in Biomedicine*. 2014, vol. 27, issue 7, s. 817-825. DOI: 10.1002/nbm.3124.
- [4] Jiřík R, Souček K, Mézl M, Bartoš M, Dražanová E, Dráfi F, Grossová L, Kratochvíla, J, Macíček O, Nylund K, Hampl A, Gilja O, Taxt T, Starčuk Z. Blind Deconvolution in Dynamic Contrast-Enhanced MRI and Ultrasound. In *36th Annual International Conference of the IEEE Engineering in Medicine and Biology Society*. 2014. p. 4276 - 4279. ISBN 978-1-4244-7929-0.